Molecular Psychiatry (2003) 8, 524–535

www.nature.com/mp

ORIGINAL RESEARCH ARTICLE

Novel truncated isoform of SK3 potassium channel is a potent dominant-negative regulator of SK currents: implications in schizophrenia

H Tomita[1,2,*], VG Shakkottai[1,*], GA Gutman[1,3], G Sun[1], WE Bunney[2], MD Cahalan[1], KG Chandy[1,†] and JJ Gargus[1,4,†]

[1]*Departments of* [1]*Physiology and Biophysics,* [2]*Psychiatry and Human Behavior,* [3]*Microbiology and Molecular Genetics,* [4]*Pediatrics, Division of Human Genetics, University of California, Irvine, CA, USA*

The small-conductance calcium-activated K^+ channel SK3 (SKCa3/KCNN3) regulates electrical excitability and neurotransmitter release in monoaminergic neurons, and has been implicated in schizophrenia, ataxia and anorexia nervosa. We have identified a novel SK3 transcript, SK3-1B that utilizes an alternative first exon (exon 1B), but is otherwise identical to SK3. SK3-1B, mRNA is widely distributed in human tissues and is present at 20–60% of SK3 in the brain. The SK3-1B protein lacks the N-terminus and first transmembrane segment, and begins eight residues upstream of the second transmembrane segment. When expressed alone, SK3-1B did not produce functional channels, but selectively suppressed endogenous SK3 currents in the pheochromocytoma cell line, PC12, in a dominant-negative fashion. This dominant inhibitory effect extended to other members of the SK subfamily, but not to voltage-gated K^+ channels, and appears to be due to intracellular trapping of endogenous SK channels. The effect of SK3-1B expression is very similar to that produced by expression of the rare SK3 truncation allele, SK3-Δ, found in a patient with schizophrenia. Regulation of SK3 and SK3-1B levels may provide a potent mechanism to titrate neuronal firing rates and neurotransmitter release in monoaminergic neurons, and alterations in the relative abundance of these proteins could contribute to abnormal neuronal excitability, and to the pathogenesis of schizophrenia.
Molecular Psychiatry (2003) **8,** 524–535. doi:10.1038/sj.mp.4001271

Keywords: Potassium channel; SKCa3; KCNN3; Schizophrenia; alternative transcript.

Introduction

A neuronal action potential is followed by an after-hyperpolarization current (I_{AHP}) which regulates spike frequency.[1,2] Fast, medium and slow components of I_{AHP} are distinguished, the fast component being mediated by large-conductance calcium-activated K^+ channels, while small-conductance calcium-activated K^+ (SK) channels are thought to be responsible for the medium, and possibly the slow components of this current.[1,2] Functional SK channels are formed from the homo- or heterotetrameric-association of products of three related genes, *SK1-SK3* (also known as *KCNN1-KCNN3* and *SKCa1–SKCa3*).[3]

Several lines of evidence have implicated the SK3 channel in schizophrenia, and more recently in anorexia nervosa[4] and ataxia,[5] although the results are not conclusive. The *SK3* gene is located on human chromosome 1q21[6] in a region containing a major susceptibility locus for familial schizophrenia[7–9] and familial hemiplegic migraine associated with permanent cerebellar ataxia.[10,11] SK3 is expressed abundantly in the regions implicated in schizophrenia[12–17] including the hippocampus, the limbic system and midbrain regions rich in monoaminergic neurons.[18–21] The SK3 channel functions as the intrinsic pacemaker in rat dopaminergic neurons,[20] and specific pharmacological blockade of SK channels abolishes the medium I_{AHP} leading to bursting action potentials and increased dopamine release,[21–26] consistent with the dopamine model of schizophrenia. SK3 contains two polymorphic polyglutamine repeats in its N-terminus. Multiple association studies find over-representation of longer alleles of the second SK3 polyglutamine repeat in schizophrenia patients,[6,27–32] although other such studies have failed to confirm this association.[33–40] SK3-Δ, a rare truncation mutant of SK3 identified in a patient with

Correspondence: Dr JJ Gargus MD, PhD Department of Physiology and Biophysics, Sprague Hall, Room 328, 39 Medical Sciences Court, University of California, Irvine CA92697-4034, USA. E-mail: jjgargus@uci.edu
*Contributed equally and are considered co-first authors.This study was supported by NIH grant MH59222 (KGC, JJG, MDC), Trousdale fellowship (HT), AHA pre-doctoral fellowship (VGS).
†These two authors are considered co-senior authors.
Received 27 June 2002; revised 2 June 2002; accepted 4 September 2002

schizophrenia,[41] potently suppressed the entire family of endogenous SK currents in mammalian cells in a dominant-negative fashion.[42] Such dominant-inhibitory behavior in dopaminergic pathways of the nervous system should have functional consequences similar to pharmacological blockade of SK channels:[24,43] bursting action potentials and increased dopamine release. Under the dopamine model of schizophrenia, such changes would predispose to the development of disease.[12,14]

Since the rare *SK3-Δ* allele suggested a powerful mechanism of SK channel modulation and neuropathogenesis, we sought to determine if there exist other more common *SK3* transcripts that might exhibit similar functional effects. Here, we describe a novel *SK3* transcript, *SK3-1B*, that is present in normal human brain at ~15–60%, the level of native full-length *SK3* mRNA. Like *SK3-Δ*, the *SK3-1B* transcript encodes a truncated protein that silences endogenous SK currents in a dominant-negative fashion by altering the distribution of SK proteins. Therefore, alterations in the abundance of this common SK3-1B protein may produce effects functionally similar to those produced by the rare *SK3-Δ* mutation.

Materials and methods

5′ RACE and determination of genomic organization

The sequence of the *SK3-1B* cDNA was extended by 5'-RACE (Rapid Amplification of cDNA Ends) with an AP1 primer (Clontech, Palo Alto, CA, USA) and an *SK3-1B*-specific primer (5′-CCTCCATCTCCACTCCCTCTGGGAGGG-3′), using human adult Marathon-ready™ cDNA (Clontech) as the template. Subsequently, a nested PCR was carried out using the RACE product and an *SK3-1B*-specific primer (5′-CCCCTCCTCCGTCTTGGGGC-3′) and an AP2 primer (Clontech). The longest product (338 bp) was purified using a QIAQuick™ gel extraction kit, ligated into PCR 2.1 vector and sequenced.

Preparation of total RNA and real-time quantitative RT-PCR

Human total RNA master panel (Clontech) was used to profile the expression pattern of *SK3-1B*. Total RNA was isolated from nine brain regions of human adult brain tissue using TRIZOL reagent (Life Technologies, Inc.) as per the manufacturer's protocol. Total RNA (1 μg) was used as a template for first-strand cDNA synthesis using poly-T primers (TaqMan reverse transcription reagents, Applied Biosystems). The mRNA for each *SK3* transcript was measured by real-time quantitative RT-PCR using a Prism model 7700-sequence detection instrument (PE Applied Biosystems). Forward and reverse primers, and TaqMan™ fluorescent probes were designed by Primer Express version 1.5 (Applied Biosystems). Forward primers were designed to anneal to sequences unique to the distinct initial exons of the two *SK3* transcripts. The sequences of forward primers were 5′-TGTTATGGTGATAGAGACCGAGCTC-3′ for *SK3* and 5′-AGCCCCAAGACGGAGGAG-3′ for *SK3-1B*. The reverse primers, designed to anneal to sequences in the shared exon 2, were 5′-TGGACAGACTGATAAGGCATTTCA-3′ for *SK3* and 5′-GGCCAACGAAAACATGGAGT-3′ for *SK3-1B*. The TaqMan™ fluorescent probes (5′-labeled with 6FAM, and 3′-labeled with TAMRA as a quencher), designed to anneal to sequences between the forward and reverse primers, were 5′-TGTACTCAAAGGACTCCATGTTTTCGTTGGC-3′ for *SK3* and 5′-TCCCAGAGGGAGTGGAGATGGAGGA-3′ for *SK3-1B*. The *SK3* and *SK3-1B* amplification products were 92 and 76 bp, respectively. The threshold cycle, C_t, which correlates inversely with the target mRNA levels, was measured as the cycle number at which the reporter fluorescent emission increased above a pre-set threshold level. To obtain absolute quantification, standard curves were plotted for every assay and were generated using defined concentrations of *SK3-1B* in Image clone 4139388, and *SK3* cDNA cloned in pcDNA3.1 HisB. Standard curves for each amplicon were plotted from eight different concentrations of standards, each run in triplicate. Concentrations were determined by spectrophotometry and purity confirmed by agarose gel electrophoresis. Purified clones were diluted to eight different concentrations and stored in single-use aliquots at −20°C, and the same diluted preparations were used throughout.

GFP constructs

Expressible constructs of the SK3 channel isoforms were produced with C-terminal GFP fluorescent tags to allow facile identification of expressing cells for electrophysiological recording. By inserting in-frame the *SK3-1B* coding region upstream to GFP in the *pEGFP-N1* expression vector (Clontech), we generated *SK3-1B-GFP*. We also generated an SK3-1B construct containing GFP driven by an internal ribosome entry site (*SK3-1B-IRES-GFP*) by inserting the *SK3-1B*-coding region into the *pIRES2-EGFP* expression vector (Clontech). The generation of the GFP-tagged Kv1.7 construct and the electrophysiological characterization of this tagged channel have been previously described.[44]

Cell culture

PC12 cells and Jurkat T lymphocytes were obtained from ATCC (Manassas, VA, USA). PC12 cells were cultured in Dulbecco's modified Eagle's medium containing 10% fetal calf serum and 2 mM glutamine in a 37°C humidified incubator with 5% CO_2 and split 1:10 twice weekly. Jurkat T lymphocytes were cultured in RPMI containing 10% fetal calf serum, 2 mM glutamine and RPMI vitamins. Cells were split 1:4 every 2 days. Unless otherwise specified, all reagents were obtained from Sigma.

Transfection of constructs into PC12 and Jurkat cells
PC12 cells were plated in 12-well plates (5×10^5 cells/chamber) for 12–24 h, and then transiently transfected using FuGene™ 6 (Roche Molecular Biochemicals, Indianapolis, IN, USA) with the DNA construct of interest in serum-free OptiMEM medium (Life Technologies, Inc.) as per the manufacturer's recommended protocol. Cells were plated 36 h following transfection for overnight growth on glass coverslips and used for electrophysiological, immunolabeling and confocal microscopy experiments 48 h post-transfection. Jurkat T lymphocytes were transiently transfected using Xtremegene-Q2 transfection reagent (Roche) as per the manufacturer's recommended protocol. Cells were used for electrophysiological analysis 48 h following transfection.

Immunostaining
Following washing with Dulbecco's phosphate-buffered saline (DPBS), cells were fixed with 4% paraformaldehyde for 20 min and washed 2 × with DPBS. Permeabilization and blocking was done with 0.2% Triton-X-100 in 10% normal goat serum, followed by a wash with DPBS. Permeabilized cells were incubated with rabbit anti-SK3 antibody (Alomone Labs, Jerusalem, Israel) in a carrier solution containing 1% normal goat serum and 0.2 % sodium azide for 4 h at 4°C. Cells were subsequently washed and incubated with 1 μg/ml Alexa-Fluor 594 (referred to as Alexa-red)-conjugated goat-anti-rabbit-IgG (Molecular Probes) for 1 h at room temperature. The secondary antibody alone showed no signal above background (data not shown). SK3 antibody specificity was confirmed by preincubation of the primary antibody for 1 h with the blocking peptide supplied by the manufacturer (data not shown). As an additional test of antibody specificity, the anti-SK3 antibody was shown not to react with SK3-1B protein, an isoform that lacks the SK3 N-terminal epitope detected by the antibody (data not shown). Cells were mounted in 50% glycerol DPBS and stored in the dark prior to microscopic analysis.

Confocal microscopy
Images were collected with an MRC-1024 laser scanning confocal microscope (Bio-Rad, Hercules, CA, USA) on an inverted Nikon Diaphot 200 stand using a 100 × oil-immersion objective (Nikon, Melville, NY, USA). Confocal sections through the cell were taken by 1 μM increments of the focus motor. Laser power was maintained at 30% for image acquisition. Excitation wavelengths of 488 and 568 nM were used, and image collection was with 522/35 and 605/32 emission filters. Images were processed with Confocal Assistant™ and Adobe™ Photoshop 5.0.2. The Scion image 4.0.2 program (Scion Corporation, Frederick, MD, USA) was used to determine the pixel intensity of fluorescence that tagged presumptive intracellular and membrane SK3 protein. Three axes were drawn through each stained cell and pixel intensities were measured along each of these axes. The cell margins were defined as a rise of pixel intensity to 50% above background. The length of the axes between the cell margins was normalized to obtain the average intensity profile for each cell. The mean of the scaled intensity histograms was obtained for six native PC12 cells and six cells transfected with each GFP construct. The average ratio of presumptive membrane to intracellular fluorescence was estimated from these intensity histograms. The expression level of each transfected construct was quantitated as mean pixel intensity.

Electrophysiology
PC12 and Jurkat T cells were studied in the whole cell configuration of the patch clamp technique with a holding potential of −80 mV. We determined SK and K_V current amplitude in untransfected cells or in cells transfected with SK3-1B-GFP, SK3-1B-IRES-GFP or control constructs (GFP vector alone, GFP-Kv1.7). We used strategies previously employed for other types of K^+ channels[42,45–48] to determine whether SK3-1B could selectively suppress endogenous SK currents without affecting K_V currents. This approach relies on the tetrameric structure of K^+ channels[49–52] and on the ability of SK subunits to coassemble specifically with other SK subunits.[3] We overexpressed SK3-1B in PC12 and Jurkat cells to ensure that the majority of SK tetramers would contain at least one SK3-1B subunit. Brightly GFP-positive cells were identified under a fluorescence microscope to allow the analysis of cells expressing high levels of the channel constructs for electrophysiological studies. Control constructs were expressed at equivalently high levels as assessed by the intensity of the GFP signal.

To activate SK channels, the pipette solution contained (in mM): 145 K^+ aspartate, 2 $MgCl_2$, 10 HEPES, 10 K_2EGTA, and 8.5 $CaCl_2$ (1 μM free Ca^{2+}), pH 7.2, 290–310 mOsm. The external solution contained (in mM): 160 K^+ aspartate (aspartate was used to minimize contributions of Cl^- current), 4.5 KCl, 2 $CaCl_2$, 1 $MgCl_2$, and 5 HEPES, pH 7.4, 290–310 mOsm. SK currents were elicited by 200-ms voltage ramps from −120 to 40 mV applied every 10 s, and slope conductance at −80 mV was taken as a measure of the SK conductance. Block of the SK current with apamin (BACHEM Bioscience Inc., King of Prussia, PA, USA) or with Lei-Dab^7 (gift from Jean-Marc Sabatier, University of Marseille) was observed as a reduction in slope conductance at −80 mV. To demonstrate the Ca^{2+} dependence of this current, we used an internal solution containing calcium-free KF. The amplitude of the K_V current was measured as the maximum current at 30 mV in 160 Na^+ aspartate. Results obtained from untransfected and transfected cells were compared using Student's *t*-test.

Results

SK3-1B lacks the N-terminus and S1 transmembrane segment

A BLAST search of GenBank with the human *SK3* AJ251016 cDNA sequence identified a novel human *SK3* EST (accession no. BF306047) derived from rhabdomyosarcoma cells. We sequenced the entire 1406 bp insert in the IMAGE clone no. 4139388 corresponding to this EST and found it to represent a novel transcript, henceforth referred to as *SK3-1B*. Using 5′ RACE on human brain mRNA with an *SK3-1B*-specific primer, we amplified and sequenced a 338 bp product and determined the approximate transcription start site of *SK3-1B*. The composite 1658 bp *SK3-1B* cDNA sequence has been deposited in GenBank (accession no. AY138900) and contains 377 bp of 5′ noncoding sequence and a 1254 bp open reading frame.

Comparison of the *SK3-1B* cDNA sequence with published genomic sequences[53] (Accession nos: AF336797, AC034149, AC027645, AC025385) revealed the intron–exon organization of *SK3-1B* (Figure 1a). *SK3* and *SK3-1B* both utilize exons 2–8 and differ only at the 5′ end (Figure 1a). Whereas *SK3* reads through the entire first exon (exon 1A) and then splices into exon 2,[53] *SK3-1B* utilizes a novel exon (exon 1B) located 712 bp downstream from exon 1A, which splices to exon 2 (Figure 1a, b). Exon 1B sequence has been deposited in GenBank and assigned accession no. AY138901. The splice donor and acceptor sites at the boundaries of the intervening sequences between exons 1, 1B and 2 are shown in Figure 1b. Exon 1A encodes the 5′ noncoding sequence, the entire N-terminus and the S1 transmembrane domain of SK3, while exon-1B encodes only the 5′ noncoding sequence of SK3-1B; the initiation codon for the SK3-1B isoform is contained in exon 2.

The putative protein products of *SK3* and *SK3-1B* are shown in Figure 1c. The SK3 protein (736 residues) is made up of a long N-terminus containing two polymorphic polyglutamine repeats, six transmembrane segments (S1–S6) and a C-terminus tightly

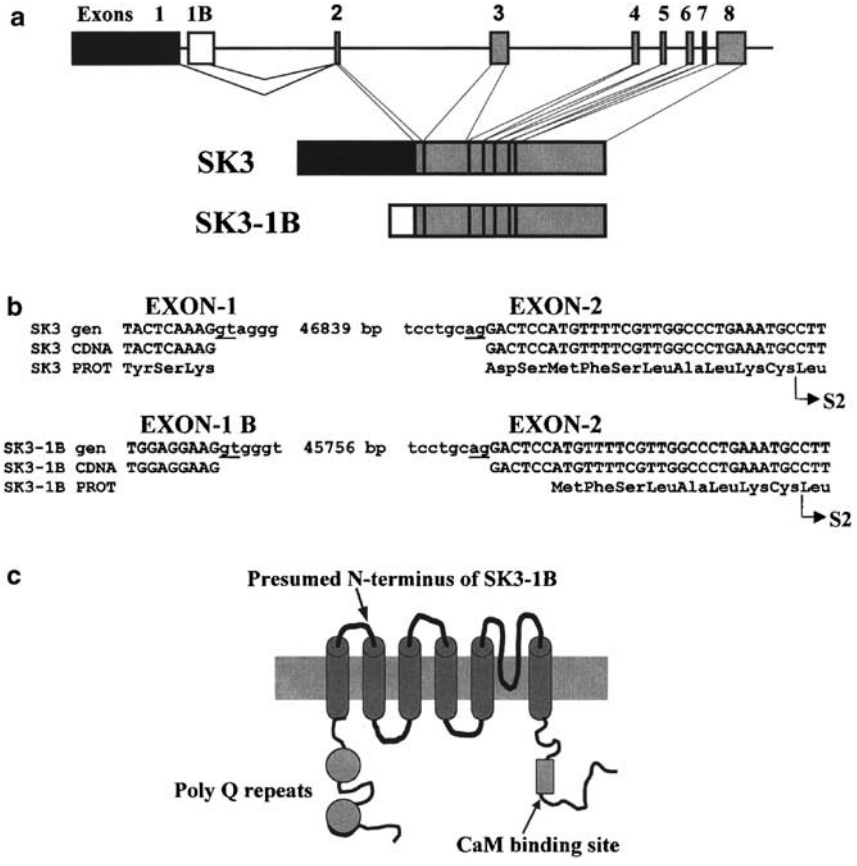

Figure 1 Genomic organization, splice junctions and putative protein products of SK3 and SK3-1B. (a) Exon–intron organization of the SK3 locus showing the location of exon 1B. The SK3 and SK3-1B cDNAs are shown below (not to scale). (b) 5′ and 3′ boundaries of the introns that lie between exons 1, 1B and 2. The AUG shown in the SK3-1B protein was determined by the NetStart1.0 (www.cbs.dtu.dk/services/Netstart) program (score 0.590; score >0.5 being significant) to be a reasonable translation initiation codon. There are no in-frame potential translation start sites upstream. An in-frame AUG that corresponds more closely to the Kozak consensus sequence (score 0.752) lies 132 bp downstream to the AUG shown, and if utilized would produce an ORF of 1122bp. (c) Putative protein product of SK3 showing transmembrane segments, the calmodulin (CAM)-binding site in the C-terminus, and the polyglutamine repeats in the N-terminus. An arrow indicates the presumed start site of SK3-1B.

complexed to calmodulin. In contrast, the putative SK3-1B protein (418 residues) begins in the same reading frame as SK3, but at the first methionine residue encoded by exon 2, eight residues upstream of the S2 transmembrane segment. It therefore lacks SK3's N-terminus and S1 segment (Figure 1b).

SK3-1B is widely expressed in the human brain

TaqMan™ quantitative RT-PCR was used to determine the abundance of *SK3* and *SK3-1B* transcripts in total RNA derived from tissues pooled from multiple human donors (Clontech). Each cDNA sample was analyzed 3–9 times and the mean copy number (±SD) per microliter of cDNA determined (Figure 2). We have arbitrarily divided the expression levels into three groups (defined by horizontal lines in Figure 2a, b), *abundant* (>1000 copies/μl cDNA), *intermediate* (100–1000 copies/μl cDNA) and *low* (<100 copies/μl cDNA). *SK3* is expressed abundantly in adult and fetal brain and uterus, at intermediate levels in skeletal muscle, spleen, thymus, adrenal gland, thyroid, kidney, testis, trachea, and at low levels in bone marrow, fetal and adult liver, heart, lung, placenta, salivary gland and prostate (Figure 2a). *SK3-1B* is present abundantly in the adult brain, at intermediate levels in fetal brain, cerebellum and uterus, and at lower levels in all the other tissues studied (Figure 2b). The ratio of *SK3-1B/SK3*, displayed as a percentage, is shown in Figure 2c and 2f. In the brain *SK3-1B* is present at between 20 and 60% of the level of *SK3*, and at significantly lower levels in most other tissues.

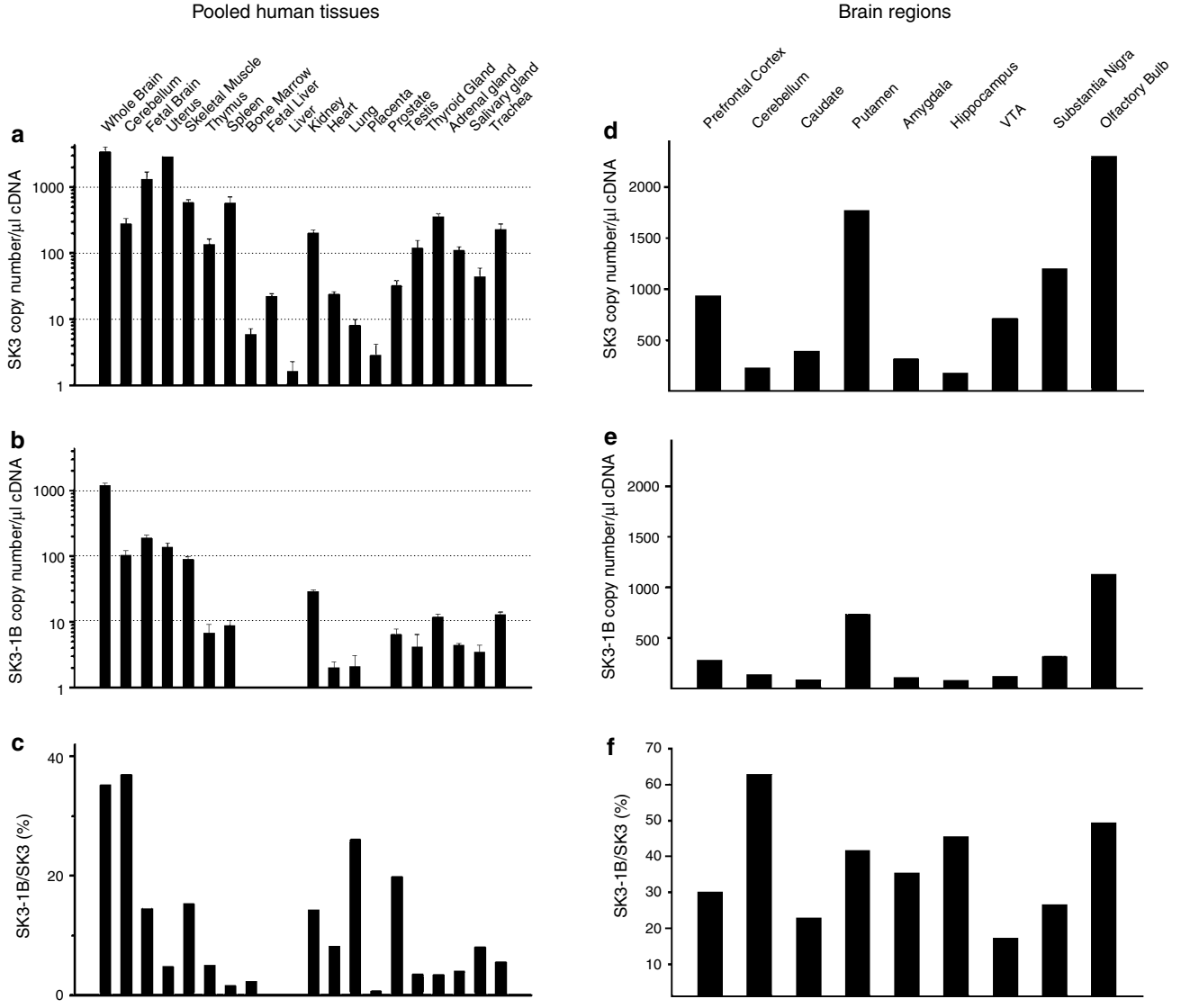

Figure 2 Distribution of SK3 and SK3-1B mRNA in human tissues determined by Taqman™ quantitative RT-PCR. (a–c) Pooled human tissues. (d–f) brain regions from a single donor. *SK3* (a, d) and *SK3-1B* (b, e) mRNA copy number per microliter cDNA expressed as mean±SD. (c, f) *SK3-1B/SK3* ratio displayed as a percentage. The horizontal lines in (a) and (b) show the arbitrary division into abundant, intermediate and low expression levels. TA: Ventral tegmental area. *No detectable transcript.

TaqMan™ RT-PCR was also performed on *SK3* and *SK3-1B* products amplified from total RNA isolated from different brain regions of a single human donor (Figures 2d–f). *SK3* was highly expressed in the olfactory bulb, putamen, prefrontal cortex, and in dopaminergic neurons in the ventral tegmental area and substantia nigra, and at lower levels in the caudate, amygdala, hippocampus and cerebellum (Figure 2d), findings consistent with published expression data [6,18,19]. *SK3-1B* was present in all these regions although at lower levels than *SK3* (Figure 2e). The ratio of *SK3-1B/SK3* in the different brain areas of this donor varied from 20 to 60% (Figure 2f). The high ratio of *SK3-1B/SK3* in the pooled brain sample is consistent with the overall levels found in the single donor brain regions (cf Figure 2c with f).

SK3-1B-GFP selectively suppresses endogenous SK currents in PC12 cells in a dominant-negative manner

GFP-tagged SK3 produces calcium-activated apamin-sensitive potassium currents when expressed in COS-7 cells,[54,55] whereas SK3-1B-GFP exhibited no channel function when expressed alone (data not shown). Since the SK3-Δ truncation mutant[42] and an N-terminal SK2 fragment[47] were both reported to suppress SK currents in mammalian cell lines, presumably by coassembling with endogenous SK subunits into nonfunctional tetramers, we tested whether SK3-1B could exhibit similar dominant-inhibitory activity. In support of this idea, protein fragments of K_V and IK K^+ channels corresponding to the region contained in SK3-1B have been shown to suppress K_V and IK currents.[45,46] We chose the rat pheochromocytoma cell line, PC12, as our experimental system since these cells natively express SK3 currents,[53] as well as K_V currents that would serve as an internal control. Two SK3-1B constructs were used: SK3-1B-GFP and SK3-1B-IRES-GFP. As controls, we expressed GFP alone or an unrelated GFP-tagged channel (GFP-Kv1.7). The expression level of each construct was quantitated as mean pixel intensity. SK3-1B-GFP was expressed at a slightly lower

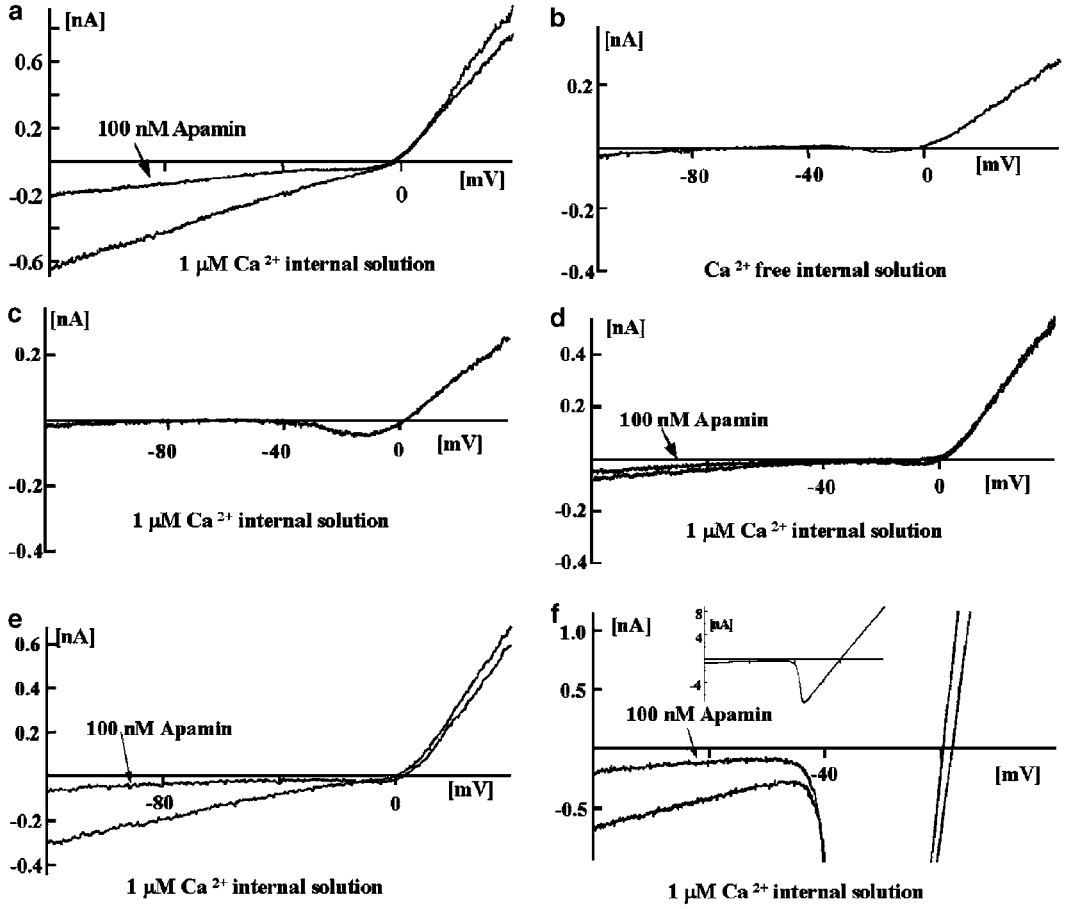

Figure 3 Dominant negative suppression of endogenous SK currents in PC12 cells by SK3-1B. SK and K_V currents in untransfected PC12 cells. Activation of SK current in PC12 with 1 μM Ca^{2+} in the internal solution; K_V currents are visible at depolarized potentials. (a) SK but not K_v current is blocked by 100 nM apamin. **(b)** In the absence of internal Ca^{2+} in the pipette solution, SK currents are not visible but K_v currents remain unchanged. SK3-1B-GFP **(c)** and SK3-1B-IRES-GFP **(d)** suppress SK but not K_v currents. GFP- **(e)** and GFP-Kv1.7 **(f)** do not affect SK and K_V currents. All SK recordings were done with symmetric (160 mM) K^+ as internal and external recording solutions. K_V current amplitude was determined with an external solution containing 160 mM Na^+ aspartate.

level (mean pixel intensity 108) than GFP-Kv1.7 (mean pixel intensity 180) or GFP vector alone (mean pixel intensity 174).

Figure 3a demonstrates the endogenous SK3 and K_V currents in PC12 cells. Current traces were elicited by voltage ramps from −80 to 40 mV. At potentials more negative than −40 mV, an inward SK3 current was seen if the pipette contained 1 μM free calcium (Figure 3a), but was absent when calcium was omitted from the pipette solution (Figure 3b). The calcium-activated inward SK3 current was selectively blocked by apamin (100 nM), a potent peptide blocker of SK channels (Figure 3a). The outward apamin sensitive K_V current observed at potentials more positive than 0 mV was unaffected by the internal calcium concentration (Figure 3a,b). The amplitudes of the SK3 and K_v currents varied from cell to cell and are summarized in Figure 4.

Expression of GFP-tagged SK3-1B (SK3-1B-GFP) in PC12 cells abolished the native SK3 current without affecting the endogenous K_v current (cf Figure 3c with a). Untagged SK3-1B in a bicistronic vector containing GFP under translational control of an IRES element (SK3-1B-IRES-GFP) had a similar suppressive effect (Figure 3d). To control for possible artifacts due to transfection and GFP overexpression, patch clamp experiments were performed on PC12 cells transfected with the GFP vector alone. SK currents in GFP-transfected cells were sensitive to apamin and of comparable amplitude to untransfected cells (cf Figure 3e with a). Patch-clamp experiments were also performed on PC12 cells transfected with a GFP-tagged voltage-gated potassium channel, Kv1.7, only distantly related to SK channels, to ensure that dominant-negative suppression by SK3-1B was specific (Figure 3f). In these cells, a large Kv1.7 current was seen, which was inward at –40 to 0 mV, and outward beyond 0 mV, consistent with the Nernst potential for potassium. Despite the presence of this substantial K_v current, the amplitude of the apamin-sensitive SK currents (seen at potentials more negative than −40 mV) was indistinguishable from controls. The scatter plot in Figure 4 summarizes the data and demonstrates that SK3-1B-GFP and SK3-1B-IRES-GFP selectively suppress endogenous SK currents without affecting K_V currents (means ± SEM in Figure 4 legend). Together, these results indicate that SK3-1B suppresses native SK currents in PC12 cells specifically and in a dominant-negative fashion.

SK3-1B suppresses other SK channels in a dominant-inhibitory manner

We next determined whether SK3-1B could suppress SK2 channels. We chose the human Jurkat T lymphocyte line for these experiments because they express SK2 channels and no other SK channels, along with voltage-gated Kv1.3 channels that could serve as an internal control.[47,56,57] Using the electrophysiological protocol described above for PC12 cells, we measured SK2 and Kv1.3 currents in Jurkat cells. The inward SK2 current, detected at potentials more negative than −40 mV, was blocked by Lei-Dab^7 (Figure 5a), a highly specific SK2 peptide inhibitor.[55] Consistent with the Nernst potential for potassium, the Kv1.3 current was inward between −40 and 0 mV, and outward beyond 0 mV, and was unaffected by Lei-Dab^7 (Figure 5a). The native SK2 current was

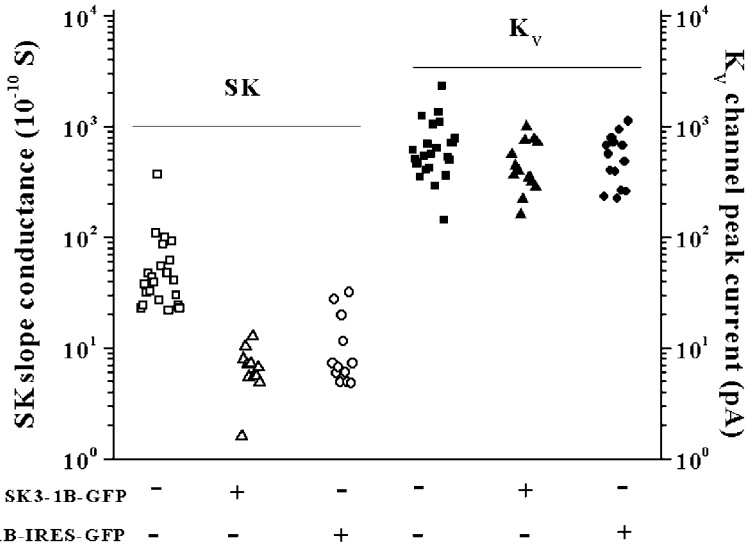

Figure 4 Scatter plot showing the effect of SK3-1B-GFP and SK3-1B-IRES-GFP on endogenous SK and K_v currents in PC12 cells. SK currents (mean ± SEM) in untransfected (open squares; 6.24 ± 1.57 nS, $n = 22$), SK3-1B-GFP-transfected (open triangles, 0.68 ± 0.08 nS, $n = 11$; $p = 0.018$) and SK3-1B-IRES-GFP-transfected PC12 cells (open circles; 1.1 ± 0.03 nS, $n = 12$; $p = 0.024$). K_v currents (mean ± SEM) in untransfected (filled squares; 707.94 ± 147.7 pA, $n = 15$), SK3-1B-GFP-transfected (filled triangles; 475.96 ± 61.78 pA, $n = 15$; $p > 0.05$) and SK3-1B-IRES-GFP-transfected PC12 cells (filled circles; 560.37 ± 75.9 pA, $n = 14$; $p > 0.05$). The data were analyzed by a Student's *t*-test between the respective transfected cell population and the untransfected PC12 cells.

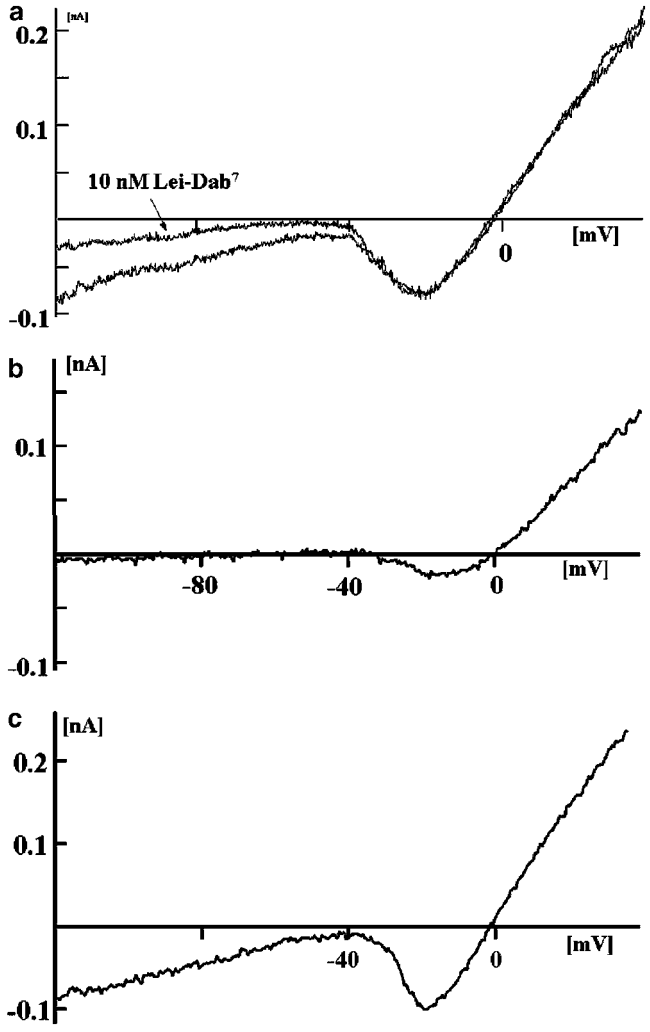

Figure 5 Dominant negative suppression of endogenous SK2 currents in Jurkat T lymphocytes by SK3-1B. (a) SK2 and Kv1.3 currents in untransfected Jurkat T lymphocytes; SK2 but not Kv1.3 is blocked by 100 nM Lei-Dab^7. **(b)** SK2 and Kv1.3 currents in SK3-1B-GFP-transfected Jurkat T lymphocytes; no SK2 current is observed ($n=4$), while the Kv1.3 current resembles that in untransfected cells. **(c)** SK2 and Kv1.3 currents in GFP-transfected Jurkat T lymphocytes ($n=4$). All experiments were done with symmetric (160 mM) K^+ as internal and external recording solutions.

suppressed by SK3-1B, while the control Kv1.3 current was unaffected (Figure 5b). This effect was specific since transfection of the GFP vector alone had no effect on either current (Figure 5c). The ability of SK3-1B to suppress channels composed of SK3 and SK2 subunits suggests a potent form of negative dominant inhibition that may affect an entire subfamily of K^+ channels, a channel family known to play a key role in regulating neuronal electrical firing frequency.

Dominant-negative suppression by SK3-1B sequesters native SK3

We performed immunolabeling and confocal microscopy experiments on PC12 cells to discern whether SK3-1B's dominant inhibitory effect was due to its ability to alter the subcellular localization of native SK3. A Nomarski image of a PC12 cell is shown in the upper panel of Figure 6a. Endogenous SK3 protein was identified in this cell with an antibody that reacts only with the N-terminus of the full-length SK3 protein[20] followed by a fluorescent (Alexa-594 conjugated) red secondary antibody. SK3 staining exhibited an annular pattern consistent with cell membrane expression (Figure 6a, middle panel). Using Scion image software, we determined the pixel intensity of presumptive membrane and intracellular SK3 fluorescence, and the average intensity histogram is shown in the lower panel of Figure 6a.

The subcellular localization of endogenous SK3 changed significantly following transfection of SK3-1B-GFP (cf Figure 6b with a). In cells expressing SK3-1B-GFP (Figure 6b, upper panel), native SK3 exhibited a red intracellular speckled pattern with diminished fluorescence intensity at the cell periphery (Figure 6b, middle panel). The average intensity histogram of SK3 fluorescence (Figure 6b, lower

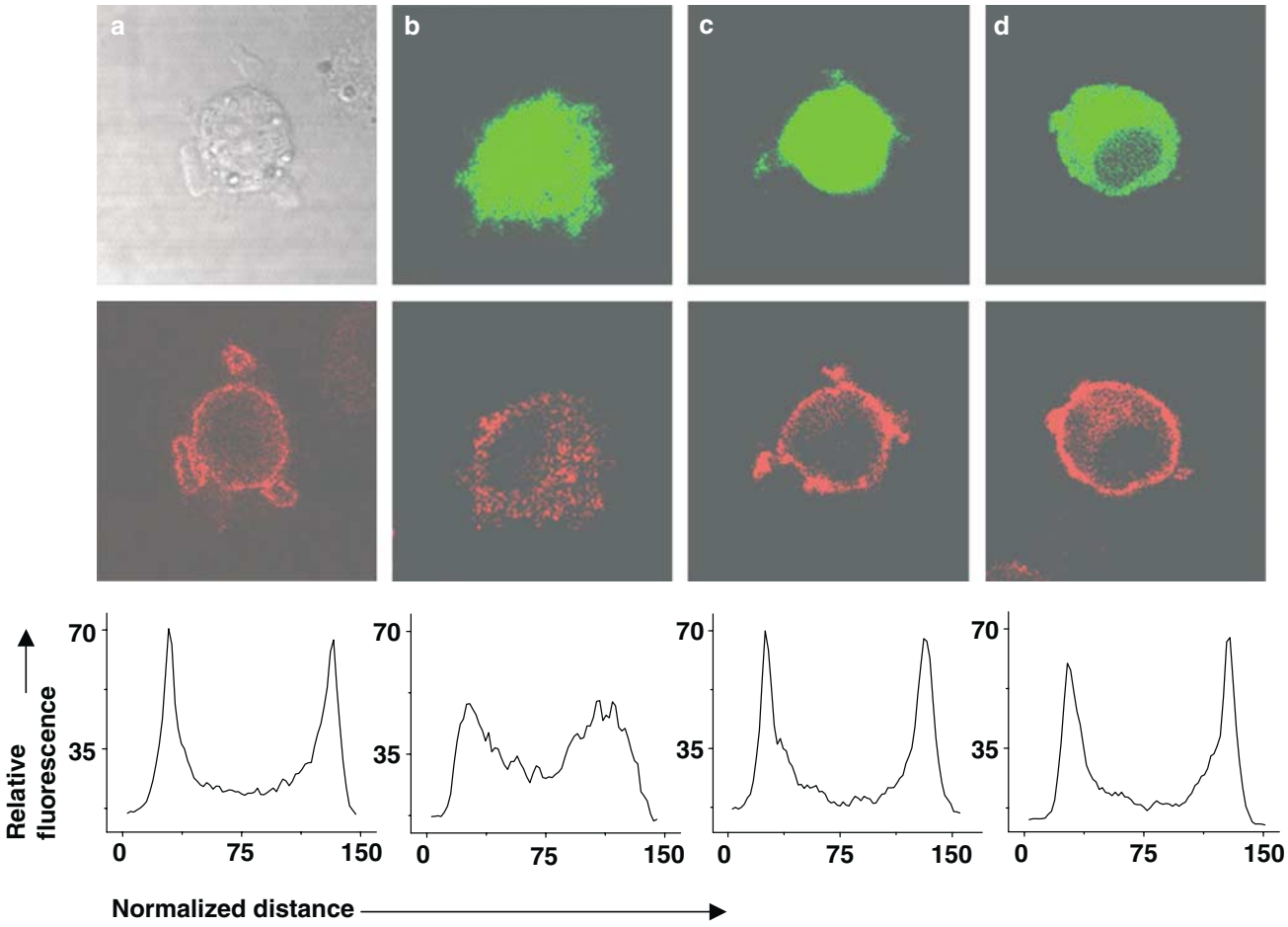

Figure 6 Altered sub-cellular expression pattern of native SK3 in PC12 cells transfected with SK3-1B. (a) Untransfected PC12 cells immunolabeled with anti-SK3 antibody; Nomarski image (upper panel), annular SK3 staining pattern (middle panel), intensity histogram of SK3 fluorescence (lower panel). Pre-incubation with blocking peptide abolished staining confirming the specificity of the antibody (data not shown). **(b)** SK3-1B-GFP-transfected cells stained for SK3; SK3-1B-GFP (upper panel), intracellular speckled SK3 staining (middle panel), intensity histogram of SK3 fluorescence (lower panel). The anti-SK3 antibody does not react with SK3-1B, which lacks the SK3 N-terminus (data not shown). (c) GFP-vector transfected cell; GFP (upper panel), annular SK3 staining (middle panel), and intensity histogram of SK3 fluorescence resembles that of untransfected cells (lower panel). **(d)**. GFP-Kv1.7-transfected cell: GFP-Kv1.7 (upper panel), annular SK3 staining (middle panel) and normal intensity histogram (lower panel). The average intensity histograms shown are based on data derived from six cells.

panel) was strikingly different from that of the native channel in untransfected cells. The sharp peaks evident in untransfected PC12 (lower panel, Figure 6a) reflect the predominantly annular distribution of the native SK3 channel protein. In contrast, in *SK3-1B* transfected cells, a greater proportion of the native SK3 protein is located intracellularly (lower panel, Figure 6b). To control for nonspecific effects we used the same constructs used in the electrophysiology studies: GFP vector alone (Figure 6c) or GFP-tagged Kv1.7 (Figure 6d). These control constructs were expressed at a higher level (mean pixel intensity 170–180) than SK3-1B (mean pixel intensity: 108). Although GFP- and GFP-Kv1.7 transfected cells showed some degree of intracellular speckling (middle panels, Figure 6c, d), the pattern was predominantly annular and the average intensity histogram data from multiple cells (lower panels, Figure 6c, d) were similar to untransfected cells (lower panel, Figure 6a). We estimated the ratio of presumptive membrane to intracellular SK3 fluorescence from the intensity histograms. The ratio in SK3-1B-GFP-transfected PC12 cells (1.1 ± 0.09; mean $\pm$ SEM) was significantly different ($p < 0.001$) from that in untransfected cells (1.72 ± 0.08) or in cells transfected with GFP vector (1.98 ± 0.09) or GFP-Kv1.7 (1.76 ± 0.09). These results taken together with the electrophysiological analysis suggest that SK3-1B achieves dominant-negative inhibition of endogenous SK currents in PC12 and Jurkat cells by decreasing the abundance of functional channels in the plasma membrane, possibly by selectively coassembling with and sequestering native SK protein in intracellular compartments.

Discussion

We have identified a novel SK3 transcript, SK3-1B, that is generated by alternate utilization of a novel exon, exon 1B, instead of exon 1. Quantitative RT-PCR experiments revealed SK3-1B expression in the brain at levels 20–60% of those of SK3. The SK3-1B mRNA encodes a 418 amino-acid-long truncated protein that begins just upstream of the second transmembrane span, S2, and is identical to SK3 from that point to the C-terminal end. SK3-1B did not produce functional channels, but instead specifically suppressed endogenous SK currents *in vitro* (SK3 current in PC12 cells and SK2 current in Jurkat cells) in a family-wide dominant-negative fashion without affecting native K_V currents. Immunolabeling and confocal microscopy studies suggest that SK3-1B's dominant-inhibitory activity is due to decreased numbers of functional SK channels in the plasma membrane, possibly due to trapping of native SK proteins in intracellular compartments. In both regards, the dominant-inhibitory activity of SK3-1B resembles that of the truncated SK3 mutant, SK3-Δ, isolated from a patient with schizophrenia.[42] These results further suggest a potent, family-wide, dominant-negative mechanism whereby variations in the levels of SK3-1B may in a consolidated manner modulate the number of functional SK channels in cells.

The human genome initiative has highlighted the importance of alternate transcripts in contributing to much of human genetic diversity and complexity,[58,59] and this is likely to be reflected in physiological systems. Some previously described disease-associated mutations in K^+ channels have come to be recognized to be pathogenic because they produce truncated nonfunctional dominant inhibitory subunits. Such mutations in *KCNQ1 (KvLQT1)*[60] and *KCNH2 (hERG)*[61] genes were recognized to produce dominant 'channelopathies' underlying Long QT syndromes. Similar mutants that truncate *KCNQ2* and *KCNQ3* are responsible for benign familial neonatal convulsion (BFNC) types 1 and 2.[62] More recently, physiological, naturally occurring mRNAs that encode 'non-functional' channel variants have shown the same potential for dominant-negative regulation of channel function. Native cardiac transcripts encoding truncated versions of the human KCNQ1 channel selectively suppress KCNQ1 currents in a manner analogous to SK3-1B.[63,64] Similarly, native transcripts encoding nonfunctional variants of several other types of channels have been reported to silence their functional counterparts. These include KCNQ2,[65] Kv8.1,[66] Kv9.1 and Kv9.2,[67] and $Ca_v2.2$.[68] Such transcripts have also been seen in nonchannel signaling proteins like lymphoid enhancer factor,[69] the chemokine receptor CCR5,[70] the estrogen receptor[71] and protein kinase PKR[72]. Thus, dominant negative regulation of multimeric proteins by non-functional variants may be a general mechanism for the regulation of protein function with a proven potential to cause disease when perturbed.[60–62,69]

Modulation by SK3-1B of functional SK channel expression in the brain is likely to have significant effects on electrical excitability. Since the family of SK channels plays an important role in defining the excitability profile of a neuron, the potential value of a dominant-negative regulatory SK3-1B subunit for both homeostasis and plasticity is apparent. SK3 is abundantly expressed in monoaminergic neurons where it plays a key role as the intrinsic pacemaker[20,25,26] and in monoamine secretion.[24,43] In a fashion analogous to pharmacological blockade of SK channels,[73] suppression of SK currents in monoaminergic neurons by SK3-1B should reduce the amplitude of the I_{AHP}, resulting in increased spike frequency and neurotransmitter release. Variation in the levels of functional *vs* suppressive SK3 subunits may provide a potent endogenous mechanism to titrate neuronal firing rates. As a result of this, alterations in the relative abundance of these SK transcripts and their encoded protein products may contribute to abnormal neuronal excitability. Excess SK3-1B, in turn, would be predicted to affect dopaminergic pathways in the brain in the manner implicated in current biological models of schizophrenia.[12,14] Further, SK3 has recently been implicated in anorexia nervosa[4] and ataxia,[5] and alterations in the SK3/SK3-1B balance may contribute to the pathogenesis of these diseases as well.

References

1 Storm JF. Potassium currents in hippocampal pyramidal cells. *Prog Brain Res* 1990; **83**: 161–187.
2 Sah P. Ca^{2+}-activated K^+ currents in neurones: types, physiological roles and modulation. *Trends Neurosci* 1996; **19**: 150–154.
3 Ishii TM, Maylie J, Adelman JP. Determinants of apamin and d-tubocurarine block in SK potassium channels. *J Biol Chem* 1997; **272**: 23195–23200.
4 Koronyo-Hamaoui M, Danziger Y, Frisch A, Stein D, Leor S, Laufer N *et al*. Association between anorexia nervosa and the hsKCa3 gene: a family-based and case control study. *Mol Psychiatry* 2002; **7**: 82–85.
5 Figueroa KP, Chan P, Schols L, Tanner C, Riess O, Perlman SL *et al*. Association of moderate polyglutamine tract expansions in the slow calcium-activated potassium channel type 3 with ataxia. *Arch Neurol* 2001; **58**: 1649–1653.
6 Dror V, Shamir E, Ghanshani S, Kimhi R, Swartz M, Barak Y *et al*. hKCa3/KCNN3 potassium channel gene: association of longer CAG repeats with schizophrenia in Israeli Ashkenazi Jews, expression in human tissues and localization to chromosome 1q21. *Mol Psychiatry* 1999; **4**: 254–260.
7 Brzustowicz LM, Hodgkinson KA, Chow EW, Honer WG, Bassett AS. Location of a major susceptibility locus for familial schizophrenia on chromosome 1q21–q22. *Science* 2000; **288**: 678–682.
8 Ekelund J, Hovatta I, Parker A, Paunio T, Varilo T, Martin R *et al*. Chromosome 1 loci in Finnish schizophrenia families. *Hum Mol Genet* 2001; **10**: 1611–1617.
9 Gurling HMD, Kalsi G, Brynjohlfson J, Sigmundsson T, Sherrington R, Mankoo BS *et al*. Genomewide genetic linkage analysis confirms the presence of susceptibility loci for schizophrenia, on chromosomes 1q32.2, 5q33.2, and 8p21-22 and provides support for linkage to schizophrenia, on chromosomes 11q23.3–24 and 20q12.1–11.23. *Am J Hum Genet* 2001; **68**: 661–673.
10 Ducros A, Joutel A, Vahedi K, Cecillon M, Ferreira A, Bernard E *et al*. Mapping of a second locus for familial hemiplegic migraine to 1q21–q23 and evidence of further heterogeneity. *Ann Neurol* 1997; **42**: 885–890.

11 Cevoli S, Pierangeli G, Monari L, Valentino ML, Bernardoni P, Mochi M *et al*. Familial hemiplegic migraine: clinical features and probable linkage to chromosome 1 in an Italian family. *Neurol Sci* 2002; **23**: 7–10.
12 Farde L. Brain imaging of schizophrenia—the dopamine hypothesis. *Schizophr Res* 1997; **28**: 157–162.
13 Csernansky JG, Csernansky CA, Kogelman L, Montgomery EM, Bardgett ME. Progressive neurodegeneration after intracerebroventricular kainic acid administration in rats: Implications for schizophrenia? *Biol Psychiatry* 1998; **44**: 1143–1150.
14 Laruelle M, Abi-Dargham P. Dopamine as the wind of the psychotic fire: new evidence from brain imaging studies. *J Psychopharmacol* 1999; **13**: 358–371.
15 Heckers S. Neuroimaging studies of the hippocampus in schizophrenia. *Hippocampus* 2001; **11**: 520–528.
16 Nopoulos PC, Ceilley JW, Gailis EA, Andreasen NC. An MRI study of midbrain morphology in patients with schizophrenia: relationship to psychosis, neuroleptics, and cerebellar neural circuitry. *Biol Psychiatry* 2001; **49**: 13–19.
17 Meyer-Lindenberg A, Miletich RS, Kohn PD, Esposito G, Carson RE, Quarantelli M *et al*. Reduced prefrontal activity predicts exaggerated striatal dopaminergic function in schizophrenia. *Nat Neurosci* 2002; **5**: 267–271.
18 Stocker M, Pedarzani P. Differential distribution of three Ca^{2+}-activated K^+ channel subunits, SK1, SK2, and SK3, in the adult rat central nervous system. *Mol Cell Neurosci* 2000; **15**: 476–493.
19 Rimini R, Rimland JM, Terstappen GC. Quantitative expression analysis of the small conductance calcium-activated potassium channels, SK1, SK2 and SK3, in human brain. *Brain Res* 2000; **85**: 218–220.
20 Wolfart J, Neuhoff H, Franz O, Roeper J. Differential expression of the small-conductance, calcium-activated potassium channel SK3 is critical for pacemaker control in dopaminergic midbrain neurons. *J Neurosci* 2001; **21**: 3443–3456.
21 Stocker M, Krause M, Pedarzani P. An apamin-sensitive Ca^{2+}-activated K^+ current in hippocampal pyramidal neurons. *Proc Natl Acad Sci USA* 1999; **96**: 4662–4667.
22 Savic N, Pedarzani P, Sciancalepore M. Medium afterhyperpolarization and firing pattern modulation in interneurons of stratum radiatum in the CA3 hippocampal region. *J Neurophysiol* 2001; **85**: 1986–1997.
23 Pedarzani P, Mosbacher J, Rivard A, Cingolani LA, Oliver D, Stocker M *et al*. Control of electrical activity in central neurons by modulating the gating of small conductance Ca^{2+}-activated K^+ channels. *J Biol Chem* 2001; **276**: 9762–9769.
24 Steketee JD, Kalivas PW. Effect of microinjections of apamin into the A10-dopamine region of rats—a behavioral and neurochemical analysis. *J Pharmacol Exp Ther* 1990; **254**: 711–719.
25 Shepard PD, Bunney BS. Effects of apamin on the discharge properties of putative dopamine-containing neurons *in vitro*. *Brain Res* 1988; **463**: 380–384.
26 Ping HX, Shepard PD. Apamin-sensitive Ca^{2+}-activated K^+ channels regulate pacemaker activity in nigral dopamine neurons. *Neuroreport* 1996; **7**: 809–814.
27 Chandy KG, Fantino E, Wittekindt O, Kalman K, Tong LL, Ho TH *et al*. Isolation of a novel potassium channel gene hSKCa3 containing a polymorphic CAG repeat: a candidate for schizophrenia and bipolar disorder? *Mol Psychiatry* 1998; **3**: 32–37.
28 Bowen T, Guy CA, Craddock N, Cardno AG, Williams NM, Spurlock G *et al*. Further support for an association between a polymorphic CAG repeat in the hKCa3 gene and schizophrenia. *Mol Psychiatry* 1998; **3**: 266–269.
29 Wittekindt O, Jauch A, Burgert E, Scharer L, Holtgreve-Grez H, Yvert G *et al*. The human small conductance calcium-regulated potassium channel gene (hSKCa3) contains two CAG repeats in exon 1, is on chromosome 1q21.3, and shows a possible association with schizophrenia. *Neurogenetics* 1998; **1**: 259–265.
30 Cardno AG, Bowen T, Guy CA, Jones LA, McCarthy G, Williams NM *et al*. CAG repeat length in the hKCa3 gene and symptom dimensions in schizophrenia. *Biol Psychiatry* 1999; **45**: 1592–1596.
31 O'Donovan MC, Owen MJ. Candidate-gene association studies of schizophrenia. *Am J Hum Genet* 1999; **65**: 587–592.
32 Ritsner M, Modai I, Amir S, Halperin T, Weizman A *et al*. An association of CAG repeats at the KCNN3 locus with symptom dimensions of schizophrenia. *Biol Psychiatry* 2002; **51**: 788–794.
33 Antonarakis SE, Blouin JL, Lasseter VK, Gehrig C, Radhakrishna U, Nestadt G *et al*. Lack of linkage or association between schizophrenia and the polymorphic trinucleotide repeat within the KCNN3 gene on chromosome 1q21. *Am J Med Genet* 1999; **88**: 348–351.
34 Joober R, Benkelfat C, Brisebois K, Toulouse A, Lafreniere RG, Turecki G *et al*. Lack of association between the hSKCa3 channel gene CAG polymorphism and schizophrenia. *Am J Med Genet* 1999; **88**: 154–157.
35 Bonnet-Brilhault F, Laurent C, Campion D, Thibaut F, Lafargue C, Charbonnier F *et al*. No evidence for involvement of KCNN3 (hSKCa3) potassium channel gene in familial and isolated cases of schizophrenia. *Eur J Hum Genet* 1999; **7**: 247–250.
36 Hawi Z, Mynett-Johnson L, Murphy V, Straub RE, Kendler KS, Walsh D *et al*. No evidence to support the association of the potassium channel gene hSKCa3 CAG repeat with schizophrenia or bipolar disorder in the Irish population. *Mol Psychiatry* 1999; **4**: 488–491.
37 Tsai MT, Shaw CK, Hsiao KJ, Chen CH. Genetic association study of a polymorphic CAG repeats array of calcium-activated potassium channel (KCNN3) gene and schizophrenia among the Chinese population from Taiwan. *Mol Psychiatry* 1999; **4**: 271–273.
38 Chowdari KV, Wood J, Ganguli R, Gottesman II, Nimgaonkar VL. Lack of association between schizophrenia and a CAG repeat polymorphism of the hSKCa3 gene in a north eastern US sample. *Mol Psychiatry* 2000; **5**: 237–238.
39 Stober G, Meyer J, Nanda I, Wienker TF, Saar K, Jatzke S *et al*. hKCNN3 which maps to chromosome 1q21 is not the causative gene in periodic catatonia, a familial subtype of schizophrenia. *Eur Arch Psychiatry Clin Neurosci* 2000; **250**: 163–168.
40 Ujike H, Yamamoto A, Tanaka Y, Takehisa Y, Takaki M, Taked T *et al*. Association study of CAG repeats in the KCNN3 gene in Japanese patients with schizophrenia, schizoaffective disorder and bipolar disorder. *Psychiatry Res* 2001; **101**: 203–207.
41 Bowen T, Williams N, Norton N, Spurlock G, Wittekindt OH, Morris-Rosendahl DJ *et al*. Mutation screening of the KCNN3 gene reveals a rare frameshift mutation. *Mol Psychiatry* 2001; **6**: 259–260.
42 Miller MJ, Rauer H, Tomita H, Rauer H, Gargus JJ, Gutman GA *et al*. Nuclear localization and dominant-negative suppression by a mutant SKCa3 N-terminal channel fragment identified in a patient with schizophrenia. *J Biol Chem* 2001; **276**: 27753–27756.
43 Dawson LA, Routledge C. Differential effects of potassium channel blockers on extracellular concentrations of dopamine and 5-HT in the striatum of conscious rats. *Br J Pharmacol* 1995; **116**: 3260–3264.
44 Bardien-Kruger S, Wulff H, Arieff Z, Brink P, Chandy KG, Corfield V. Characterisation of the human voltage-gated potassium channel gene, KCNA7, a candidate gene for inherited cardiac disorders, and its exclusion as cause of progressive familial heart block I (PFHBI). *Eur J Hum Genet* 2002; **10**: 36–43.
45 Tu L, Santarelli V, Sheng Z, Skach W, Pain D, Deutsch C. Voltage-gated K^+ channels contain multiple intersubunit association sites. *J Biol Chem* 1996; **271**: 18904–18911.
46 Joiner WJ, Khanna R, Schlichter LC, Kaczmarek LK. Calmodulin regulates assembly and trafficking of SK4/IK1 Ca^{2+}-activated K^+ channels. *J Biol Chem* 2001; **276**: 37980–37985.
47 Fanger CM, Rauer H, Neben AL, Miller MJ, Rauer H, Wulff H *et al*. Calcium-activated potassium channels sustain calcium signaling in T lymphocytes. *J Biol Chem* 2001; **276**: 12249–12256.
48 Deutsch C. Potassium channel ontogeny. *Annu Rev Physiol* 2002; **64**: 19–46.
49 Doyle DA, Morais Cabral J, Pfuetzner RA, Kuo A, Gulbis JM, Cohen SL *et al*. The structure of the potassium channel: molecular basis of K^+ conduction and selectivity. *Science* 1998;**280**: 69–77.
50 Jiang YX, Lee A, Chen JY, Cadene M, Chait BT, MacKinnon R. The open pore conformation of potassium channels. *Nature* 2002; **417**: 523–526.

51 Schumacher MA, Rivard AF, Bachinger HP, Adelman JP. Structure of the gating domain of a Ca^{2+}-activated K^+ channel complexed with Ca^{2+}/calmodulin. *Nature* 2001; **410**: 1120–1124.
52 Jiang YX, Lee A, Chen JY, Cadene M, Chait BT, MacKinnon R. Crystal structure and mechanism of a calcium-gated potassium channel. *Nature* 2002; **417**: 515–522.
53 Sun G, Tomita H, Shakkottai VG, Gargus JJ. Genomic organization and promoter analysis of human KCNN3 gene. *J Hum Genet* 2001; **46**: 463–470.
54 Wulff H, Gutman GA, Cahalan MD, Chandy KG. Delineation of the clotrimazole/TRAM-34 binding site on the intermediate conductance calcium-activated potassium channel, IKCa1. *J Biol Chem* 2001; **276**: 32040–32045.
55 Shakkottai VG, Regaya I, Wulff H, Fajloun Z, Tomita H, Fathallah M *et al*. Design and characterization of a highly selective peptide inhibitor of the small conductance calcium-activated K^+ channel, SkCa2. *J Biol Chem* 2001; **276**: 43145–43151.
56 Grissmer S, Lewis RS, Cahalan MD. Ca^{2+}-activated K^+ channels in human leukemic T cells. *J Gen Physiol* 1992; **99**: 63–84.
57 Desai R, Peretz A, Idelson H, Lazarovici P, Attali B. Ca^{2+}-activated K^+ channels in human leukemic jurkat T cells. Molecular cloning, biochemical and functional characterization. *J Biol Chem* 2000; **275**: 39954–39963.
58 Southan C. A genomic perspective on human proteases. *FEBS Lett* 2001; **498**: 214–218.
59 Brett D, Pospisil H, Valcarel J, Reich J, Bork P. Alternative splicing and genome complexity. *Nat Genet* 2002; **30**: 29–30.
60 Shalaby FY, Levesque PC, Yang WP, Little WA, Conder ML, Jenkins-West T *et al*. Dominant-negative KvLQT1 mutations underlie the LQT1 form of long QT syndrome. *Circulation* 1997; **96**: 1733–1736.
61 Kagan A, Yu Z, Fishman GI, McDonald TV. The dominant negative LQT2 mutation A561V reduces wild-type HERG expression. *J Biol Chem* 2000; **275**: 11241–11248.
62 Schroeder BC, Kubisch C, Stein V, Jentsch TJ. Moderate loss of function of cyclic-AMP-modulated KCNQ2/KCNQ3 K^+ channels causes epilepsy. *Nature* 1998; **396**: 687–690.
63 Jiang M, Tseng-Crank J, Tseng GN. Suppression of slow delayed rectifier current by a truncated isoform of KvLQT1 cloned from normal human heart. *J Biol Chem* 1997; **272**: 24109–24112.
64 Demolombe S, Baro I, Pereon Y, Bliek J, Mohammad-Panah R, Pollard H *et al*. A dominant negative isoform of the long QT syndrome 1 gene product. *J Biol Chem* 1998; **273**: 6837–6843.
65 Smith JS, Iannotti CA, Dargis P, Christian EP, Aiyar J. Differential expression of kcnq2 splice variants: implications to m current function during neuronal development. *J Neurosci* 2001; **21**: 1096–1103.
66 Hugnot JP, Salinas M, Lesage F, Guillemare E, de Weille J, Heurteaux C *et al*. Kv8.1, a new neuronal potassium channel subunit with specific inhibitory properties towards Shab and Shaw channels. *EMBO J* 1996; **15**: 3322–3331.
67 Salinas M, Duprat F, Heurteaux C, Hugnot JP, Lazdunski M. New modulatory alpha subunits for mammalian Shab K^+ channels. *J Biol Chem* 1997; **272**: 24371–24379.
68 Raghib A, Bertaso F, Davies A, Page KM, Meir A, Bogdanov Y *et al*. Dominant-negative synthesis suppression of voltage-gated calcium channel cav2.2 induced by truncated constructs. *J Neurosci* 2001; **21**: 8495–8504.
69 Hovanes K, Li TW, Munguia JE, Truong T, Milovanovic T, Lawrence Marsh J *et al*. Beta-catenin-sensitive isoforms of lymphoid enhancer factor-1 are selectively expressed in colon cancer. *Nat Genet* 2001; **28**: 3–4.
70 Chelli M, Alizon M. Determinants of the trans-dominant negative effect of truncated forms of the CCR5 Chemokine Receptor. *J Biol Chem* 2001; **276**: 46975–46982.
71 Tiffoche C, Vaillant C, Schausi D, Thieulant ML. Novel intronic promoter in the rat ER alpha gene responsible for the transient transcription of a variant receptor. *Endocrinology* 2001; **142**: 4106–4119.
72 Gil J, Rullas J, Garcia MA, Alcami J, Esteban M. The catalytic activity of dsRNA-dependent protein kinase, PKR, is required for NF-kappaB activation. *Oncogene* 2001; **20**: 385–394.
73 Shepard PD, Bunney BS. Repetitive firing properties of putative dopamine-containing neurons invitro—regulation by an apamin-sensitive Ca^{2+}-activated K^+ conductance. *Exp Brain Res* 1991; **86**: 141–150.